The novel *Huntiella omanensis* mating gene, *MAT1-2-7*, is essential for ascomatal maturation

Andi M. Wilson [a*], P. Markus Wilken [a], Magriet A. van der Nest [a, b], Michael J. Wingfield [a] and Brenda D. Wingfield [a]

[a] Department of Biochemistry, Genetics and Microbiology, Forestry and Agricultural Biotechnology Institute (FABI), Faculty of Natural and Agricultural Sciences, University of Pretoria, Hatfield Campus Pretoria, 0083, South Africa

[b] Biotechnology Platform, Agricultural Research Council (ARC), Onderstepoort Campus, Pretoria, 0110, South Africa

[*] Corresponding author

AMW: andi.wilson@fabi.up.ac.za
PMW: markus.wilken@fabi.up.ac.za
MAvdN: vandernestm@arc.agric.za
MJW: mike.wingfield@fabi.up.ac.za
BDW: brenda.wingfield@up.ac.za

ABSTRACT

Sexual reproduction is a highly conserved feature of the eukaryotes, yet sexual compatibility is determined by a wide variety of mechanisms. In ascomycete fungi, sexual development is controlled by genes at the mating type (*MAT*) locus that confer either MAT1-1 or MAT1-2 mating identity. Although the locus harbours, at minimum, a single gene, the individual *MAT* loci of certain species, including *Huntiella omanensis*, encode for two or more genes. The *MAT1-2* idiomorph of *H. omanensis* is made up of *MAT1-2-1*, a primary *MAT* gene that is highly conserved in the Pezizomycotina and possesses a well-characterized DNA binding motif, the HMG-box domain. The idiomorph also harbours a novel secondary *MAT* gene, named *MAT1-2-7*, with no recognizable functional domains. In this study, we developed a transformation and CRISPR-Cas9-based genome editing protocol to characterize the *MAT1-2-7* gene with respect to its function in mating. We have shown that *MAT1-2-7* is essential for sexual reproduction and that isolates carrying the truncated *MAT1-2-7* gene are incapable of ascomatal maturation and further sexual development. *MAT1-2-7* was also shown to influence the vegetative radial growth rate of *H. omanensis*, illustrating the pleiotropic effects often associated with *MAT* genes.

KEYWORDS

1. Sexual reproduction
2. Novel secondary *MAT* gene
3. *MAT* gene characterization
4. Protoplast-based transformation
5. CRISPR-Cas9 genome editing

1. INTRODUCTION

Sexual reproduction in ascomycetes is controlled almost entirely by genes present at the mating type (*MAT*) locus. At minimum, this includes the primary *MAT* genes, *MAT1-1-1* and *MAT1-2-1* (Debuchy et al., 2010; Dyer et al., 2016). However, other secondary genes can also be present, often in a lineage-specific manner. As the nomenclature suggests, the *MAT1-1-1* gene is the defining feature of the *MAT1-1* idiomorph, while the same is true of the *MAT1-2-1* gene at the *MAT1-2* idiomorph (Turgeon and Yoder, 2000). In heterothallic, or self-sterile, fungi, a single individual can be assigned a mating type based on the genic content of its *MAT* locus, with the *MAT1-1* idiomorph conferring the MAT1-1 mating type and the *MAT1-2* idiomorph conferring the MAT1-2 mating type (Dyer et al., 2016).

At present, there is no clear definition of a *MAT* gene. This is in part due to the limited number of functional studies on these genes, particularly in non-model species, but also the fairly extensive variation in the genic content of the *MAT* locus (Debuchy et al., 2010). Some authors have classified a *bona fide* MAT protein as one that allows for internuclear recognition and that is functional only when expressed from the *MAT* locus (Arnaise et al., 1997). This definition is highly restrictive as it relies on the functional characterization of these genes as well as the ability to precisely track the expression and location of the protein during sexual reproduction. It also does not consider the many other processes involved in sexual reproduction that are not linked to recognition but remain essential for the production of recombinant offspring. Other authors define the *MAT* locus simply as a location in the genome responsible for mating, and thus a *MAT* gene is a gene that resides within this locus (Turgeon and Yoder, 2000; Wilken et al., 2017). This definition does not rely on functional characterization and is thus more relevant in non-model fungi where gene characterization has not yet been possible.

The broader, locus-dependent definition for a mating gene has led to the description of many *MAT* genes (as recently reviewed (Wilken et al., 2017)). Of these, the *MAT1-1-1* and *MAT1-2-1* genes fulfil an essential role in the mating process and are found in almost all studied species (Debuchy and Coppin, 1992; Paoletti et al., 2007; Staben and Yanofsky, 1990). They are thus considered the primary mating genes. In comparison, the secondary

MAT genes are not as well-conserved and do not always have recognizable conserved domains (Wilken et al., 2017). These genes have been named numerically in the order of their discovery in various species (Turgeon and Yoder, 2000). Thus, for example, *Cryphonectria parasitica* harbours the *MAT1-1-2* and *MAT1-1-3* genes at the *MAT1-1* idiomorph (McGuire et al., 2001); while the *MAT1-2-2* and *MAT1-2-9* genes are harboured in the *MAT1-2* idiomorphs of *Neurospora crassa* (Pöggeler and Kück, 2000) and *Fusarium fujikuroi* (Martin et al., 2011; Wilken et al., 2017), respectively.

Functional characterization of the *MAT* genes in diverse fungal species has predominantly focused on *MAT1-1-1* and *MAT1-2-1*, and in some cases, has even concentrated specifically on their functional domains. These genes have been shown to be essential for sexual reproduction in model and non-model species alike (Debuchy and Coppin, 1992; Ferreira et al., 1998; Paoletti et al., 2007; Staben and Yanofsky, 1990). The precise functions of *MAT1-1-1* and *MAT1-2-1* are also fairly well-conserved, with both primary genes often playing important roles during the initiation of sexual reproduction. However, while these genes are well-characterized, similar research is lacking with respect to the secondary *MAT* genes. The few examples that do exist include the *Fusarium graminearum MAT1-1-2* and the *Botrytis cinerea MAT1-1-5*, both of which are important for the maturation of the ascomata (Kim et al., 2012; Rodenburg et al., 2018). In addition to their role in mating, *MAT* genes can also influence other important non-mating factors, such as pathogenicity, growth and vegetative incompatibility (Lee et al., 2015; Newmeyer et al., 1973).

Huntiella omanensis, a member of the Ceratocystidaceae (de Beer et al., 2014), has recently been the topic of genomic and transcriptomic studies with respect to its sexual development (Wilson et al., 2018, 2015). MAT1-1 isolates of this fungus possess the *MAT1-1-1* and *MAT1-1-2* genes, while the MAT1-2 isolates harbour the *MAT1-2-1* and *MAT1-2-7* genes (Wilson et al., 2015). *MAT1-1-1*, *MAT1-1-2* and *MAT1-2-1* all encode proteins that are comparable to those encoded by this locus in other species and they each possess the expected functional domains associated with these proteins. In contrast, *MAT1-2-7* was first detected *in silico* and showed no similarity to any other known genes. It also encoded a protein with no recognizable functional domains (Wilson et al., 2015). Later the gene was found to be expressed during sexual reproduction despite undetectable expression levels

during the vegetative growth phase (Wilson et al., 2018). Its position in the *MAT* locus combined with its expression pattern thus suggested that this gene might have a role in the sexual process.

Huntiella moniliformis, a close relative of *H. omanensis*, possesses a significantly truncated and likely non-functional version of the *MAT1-2-7* gene (Wilson et al., 2015). Interestingly, this species undergoes unisexual reproduction, unlike the many heterothallic species found in this genus (Wilson et al., 2015). It has thus been hypothesized that *MAT1-2-7* plays a role in the regulation of sexual reproduction in these species and that its truncation in *H. moniliformis* leads, at least in part, to the homothallic behaviour observed in this species (Wilson et al., 2018). However, *H. moniliformis* also exhibits an interesting pheromone expression pattern, with a single isolate capable of producing both mating pheromones. This is unlike *H. omanensis*, which, similar to many heterothallic species, expresses these pheromones in a mating-type dependent manner (Wilson et al., 2018). It is not known whether the truncation of the *MAT1-2-7* gene, the indiscriminate pheromone expression or a combination of both has led to unisexual reproduction.

The aim of this study was to characterize the *H. omanensis MAT1-2-7* gene with respect to its involvement in sexual reproduction. Our objective was to mimic the truncation seen in the *H. moniliformis MAT1-2-7* gene to determine whether *MAT1-2-7* disruption can bring about unisexual behaviour in *H. omanensis*. This was achieved by developing a protoplast-based transformation and CRISPR-Cas9 genome editing protocol for use in the first successful genetic modification of any species within the genus *Huntiella*. The *H. omanensis MAT1-2-7* gene was confirmed as an essential mating gene that plays an important role in ascomatal maturation.

2. METHODS AND MATERIALS

2.1. Strains and culture conditions

Four wild type isolates of *H. omanensis* were used in this study, two MAT1 isolates (CMW 44436 and CMW 44437) and two MAT2 isolates (CMW 44439 and CMW 44442). Additionally, two independent *MAT1-2-7* mutant strains were derived from

the CMW 44442 MAT2 isolate (as detailed below). These isolates have been named *ΔMAT127-H1* (CMW 54810) and *ΔMAT127-H4* (CMW 54811). Unless otherwise stated, the isolates were cultured and maintained on 2% malt extract agar, supplemented with 100 $mg.L^{-1}$ thiamine hydrochloride (Sigma, St Louis, USA) and 150 $mg.L^{-1}$ streptomycin sulphate salt (Sigma, St Louis, USA) and is referred to as MEA-ST. The cultures were maintained at 22 °C in a standard light-dark cycle. These cultures have been preserved in the culture collection (CMW) of the Forestry and Agricultural Biotechnology Institute (FABI) at the University of Pretoria in South Africa.

2.2. sgRNA design, synthesis and transcription

The single guide RNA (sgRNA) is an RNA molecule that allows the Cas9 protein to recognize the genomic region of interest and allows for DNA cleavage at a targeted region (Jinek et al., 2012). It is comprised of a 20 bp region called the protospacer which corresponds to the genomic location to be targeted and a longer scaffold region that physically binds to the Cas9 protein. Together, the sgRNA and Cas9 protein form the ribonucleoprotein (RNP) which is capable of creating targeted dsDNA breaks (Gasiunas et al., 2012). The sgRNA used to target the *H. omanensis MAT1-2-7* gene (Fig. 1) was designed to adhere to the following parameters, 1) the 20 nt protospacer was found directly upstream of a 5' NGG 3' protospacer adjacent motif (PAM), a motif specifically targeted by the *Streptococcus pyogenes* Cas9 enzyme used below, 2) the sequence of the protospacer together with the PAM sequence showed no significant similarity to any other regions of the *H. omanensis* genome, 3) the sgRNA construct passed a number of RNA folding restrictions, 4) the protospacer targeted the 5' region of the gene near the point targeted for the introduction of the in-frame stop codon.

These parameters were satisfied by annotating each of the 5' NGG 3' sequences in the *MAT1-2-7* gene and filtering through the potential sgRNA constructs. Each of the PAM sequences and the adjacent 20 nt, representing the potential protospacer, were used in local BLASTn searches against the *H. omanensis* genome to detect any potential off-target effects. Those that passed these initial control steps were subjected to RNA folding analysis using the RNAfold webserver (Gruber et al., 2008), with default settings. In order for sgRNA molecules to efficiently target the correct region of the

genome and bind the Cas9 enzyme, constructs needed to have similarly structured minimal free energy and centroid secondary structures; each made up of three stem loops and five rings. The secondary structures should also have high base pairing probabilities throughout the structure, with the exception of the 5' terminal region where the protospacer is located. The sgRNA that passed all of these requirements and that targeted the most 5' region of the gene was selected for use.

The full-length sgRNA was synthesized by Twist Biosciences (San Francisco, USA) as a dsDNA molecule. This construct was then amplified using primers targeting the protospacer and scaffold sequence. The forward primer was designed to include a 5' overhang harbouring a T7 promoter (Fig. A.1). The construct was amplified using Phusion High-Fidelity DNA polymerase (ThermoFisher Scientific, Waltham, USA) following the manufacturer's instructions (Table B.1). The resulting DNA products were visualized on a 2% SeaKem® LE agarose gel (Lonza, Rockland, USA) stained with GelRed™ (Biotium, Fremont, USA) and electrophoresed at 100V for 20 min. PCR products were purified using a 6.66% G-50 Sephadex solution (Sigma, St Louis, USA) and Centri-Sep spin columns (Princeton Separations, Freehold, USA), using the manufacturer's instructions. The cleaned products were cycle-sequenced using a BigDye Terminator Cycle Sequencing Kit v3.1 (Life Technologies, Carlsbad, USA) (Table B.2).

The construct was subsequently transcribed using the HiScribe™ T7 Quick High Yield RNA synthesis kit (New England Biolabs, Ipswich, USA) in accordance with the manufacturer's instructions. This entailed incubating approximately 1μg of target DNA together with the T7 RNA polymerase at 37°C for 16 hours. The transcribed sgRNA was then visualized as above.

2.3. *In vitro* testing of sgRNA

The cleavage ability of the designed and synthesized sgRNA was tested *in vitro*. This entailed incubating a PCR product which included the target region together with the RNP complex. The PCR product was produced using FastStart Taq DNA Polymerase (Roche, Basel, Switzerland) and primers targeting an 872 bp region of the *MAT1-2-7*

gene (Fig. A.2 and Table B.3). Successful and targeted Cas9-mediated cleavage of this PCR product would yield two DNA products 737 and 135 bp in length (Fig. A.2).

The RNP was produced using the sgRNA synthesized and transcribed as described in section 2.2. above as well as the EnGen® Spy Cas9 NSL protein (New England Biolabs, Ipswich, USA) following the manufacturer's instructions (Fig. A.1). In short, a solution of 30nM sgRNA, 30nM Cas9 protein, 10X NEBuffer 3.1 and ddH_2O was prepared and incubated at 25°C for 10 min. The target DNA was added to a final concentration of 3 nM and the solution was incubated for a further 15 min at 37°C. In order to stop the reaction, 3 μg of Proteinase K (Sigma, St Louis, USA) and 2 μg of RNase A (Roche, Basel, Switzerland) were subsequently added. The reaction was incubated at room temperature for 10 min. The resulting DNA products were visualized as above.

2.4. dDNA design

Upon Cas9-induced cleavage, the cell will attempt to repair the cut, by either using non-homologous end joining or homology directed repair (Ran et al., 2013). In the latter case, a construct harbouring a sequence of interest can be provided in the form of a donor DNA (dDNA). This allows for the introduction of foreign DNA directly into the region being cut. The dDNA includes the sequence to be introduced flanked by arms that are homologous to the region being targeted by the sgRNA. In this study, the dDNA was made up of homologous arms flanking the *BclI* restriction site (5' TGA TCA 3') and a hygromycin B resistance cassette (Fig. 2). The dDNA was designed to ensure the stop codon encoded by the *BclI* site (TGA) was in frame with the coding region of the *MAT1-2-7* gene, thereby introducing a premature stop codon. The position of this stop codon was also designed to be at the same position as the premature stop codon found in the *H. moniliformis MAT1-2-7* and thus allowed the *H. omanensis MAT1-2-7* to be truncated in a manner similar to that of *H. moniliformis*. The introduction of the hygromycin B resistance cassette allowed for the selection of successfully transformed isolates.

Originally, the dDNA was designed to be inserted into a plasmid harbouring an independent hygromycin resistance cassette and thus a dDNA molecule consisting of

only the *MAT1-2-7*-homologous flanking regions and the *BclI* restriction site was synthesized by Twist Biosciences (San Francisco, USA) as a dsDNA molecule. The full length dDNA also harbouring the hygromycin B resistance cassette was thus assembled using a step-wise, overhang PCR approach (Fig. A.3, Tables B.4 – B.9). This entailed amplifying the 5' and 3' regions of the synthesized construct using primers with overhangs homologous to the sequence of the hygromycin B resistance cassette. The entire hygromycin B resistance cassette was amplified in a single reaction from the pcb1004 plasmid (Carroll et al., 1994). These resultant PCR products were then used in a single amplification reaction to produce the single, full-length dDNA construct. Each of the intermediate and final PCR products were visualized, purified and sequenced as above.

2.5. Protoplast extractions

A protoplast extraction protocol was optimized for use in *Huntiella* species using a combination of the *Magnaporthe oryzae* and other filamentous ascomycete protoplast extraction protocols (Chung and Lee, 2015; Leung et al., 1990) with a number of species-specific alterations. A mycelial plug was inoculated in 200ml of 2% (w/v) malt extract broth and allowed to grow for between 24 and 48 hours with shaking at 100 rpm at 25 °C. To harvest conidia, the resulting liquid culture was filtered through a single layer of Miracloth® (Merck, New Jersey, USA) and centrifuged at 4000 rpm for 10 mins at 4 ℃ in an Eppendorf 5810 R centrifuge. The pellet was resuspended in 200ml of 1% (w/v) malt extract broth and allowed to grow for up to 12 hours as above. The resulting germlings and young mycelial strands were harvested by centrifugation at 4000 rpm for 10 mins at 4℃, followed by resuspension in 1M sorbitol (Sigma, St Louis, USA). This solution was either used immediately in enzymatic degradation reactions or stored at -80℃.

The germlings and young mycelia were subjected to enzymatic degradation by *Trichoderma harzianum* lysing enzymes (Sigma, St Louis, USA). The enzyme concentrations, final volumes and incubation times are summarized in Table B.10. In general, 1 ml germling/mycelia solution was added to 9 ml enzyme solution and incubated at 25 ℃ with shaking at 80 rpm. The resultant protoplast suspension was

filtered through Miracloth® and then centrifuged at 3000 rpm for 10 mins. The protoplast pellet was carefully resuspended in 300ul STC buffer (20% sucrose, 50mM Tris-HCl pH 8.00 and 50mM $CaCl_2$). Protoplasts were either used immediately in transformation experiments or stored at -80 ℃.

2.6. Transformations

A single transformation reaction consisted of protoplasts, sgRNA-Cas9 RNPs and the dDNA construct. The RNP was assembled as detailed in section 2.2. above and in accordance with manufacturer's suggestions, using 3 μM solutions of each reagent. These were combined with the 1X Cas9 reaction buffer to a total volume of 12.5 μl. This solution was incubated at room temperature for 10 min.

Approximately 5 x 10^6 protoplasts, a single volume of the RNP solution and 6 μg of the dDNA construct were co-incubated on ice for 20 mins. Subsequently, a freshly prepared 30% PTC (polyethylene glycol 8000 in STC buffer) solution was slowly dripped onto the protoplast solution, creating a hydrophobic layer above the cells. This solution was incubated for a further 20 min at room temperature. An osmotic control medium (OCM- 0.3% yeast extract, 20% sucrose, 0.3% cas-amino acids) was added to the protoplast solution and incubated with shaking at 80 rpm over night at room temperature. The solution was divided into five Petri dishes and covered with OCMA medium (OCM + 1% agar) supplemented with 30 $ug.ml^{-1}$ hygromycin B from *Streptomyces hygroscopicus* (Sigma, St Louis, USA). Once set, this medium was covered with a layer of OCMA medium supplemented with 40 $ug.ml^{-1}$ hygromycin B. Single isolates that were able to grow through the top layer of medium were transferred to MEA supplemented with 50 $ug.ml^{-1}$ hygromycin B (MEA-50).

2.7. Confirmation of transformants and stability of the insert

Isolates that were capable of growth on MEA-50 were subjected to single hyphal tip isolations and transferred to MEA-ST. DNA was extracted from these isolates after five days of growth as described in previous studies (Wilson et al., 2015). Extracted DNA was subjected to PCR amplification using primers targeting the 5' and 3' integration regions as well as the entire length of the integrated dDNA construct (Fig. A.4). These

reactions were conducted using LongAmp® Taq (New England Biolabs, Ipswich, USA) according to the manufacturer's instructions (Table B.11). PCR products were visualized, purified and sequenced as above.

To ensure that the dDNA had integrated only at a single site in the genome, DNA from the two mutant isolates was subjected to Southern blot analysis. Genomic DNA (30μg per isolate per enzyme) was digested using HindIII and EcoRI (ThermoScientific, Waltham, USA), in individual reactions and in accordance with the manufacturer's instructions. Digestions were conducted at 37 °C for 16 hours and were inactivated by incubation at 80 °C (HindIII) and 65 °C (EcoRI) for 20 mins. The digested gDNA fragments were subsequently separated on a 0.75% agarose gel and electrophoresed for 90 mins at 80V in 1x TAE buffer. The subsequent DNA transfer from the gel onto a nylon membrane was conducted as previously described (Sambrook and Green, 2012). The membrane was then subjected to probe hybridization and visualization as per the manufacturer's manual (Eisel et al., 2008). In short, a DIG-labelled probe was synthesized using a PCR-approach and DIG-labelled dNTPs (Sigma, St Louis, USA, Table B.12). The probe was designed to target a short, 336 bp region of the hygromycin resistance cassette. Once the probe was hybridized to the membrane, the membrane was treated with a 1:5000 solution of anti-digoxigenin-AP (Sigma, St Louis, USA). This was followed by incubation in a 1:5 NBT/BCIP colour substrate solution (Sigma, St Louis, USA). The colour precipitation reaction was allowed to develop for 2.5 hrs, before the membrane was neutralized and washed with double distilled water.

In order to test the stability of the integration of the hygromycin cassette, the knockout strains were alternatively transferred from media supplemented with hygromycin B to media without antibiotic supplementation (Fig. A.5). This was conducted three times and each isolate was allowed to grow for three days at 25 °C before being transferred to fresh media.

2.8. Phenotypic analysis of the wild type and mutant strains

2.8.1 Mating tests

The ability of each knockout strain to produce ascomata was assessed and compared with that of the wild type isolates. Two media types were used to induce ascomatal development: MEA-ST as detailed above as well as 2% potato dextrose agar supplemented with 100 $mg.L^{-1}$ thiamine hydrochloride and 150 $mg.L^{-1}$ streptomycin sulphate salt (PDA-ST). Plates for mating tests were set up by co-incubating two isolates on a single plate, approximately 2cm apart. The plates were not wrapped closed with parafilm, which is the standard procedure when culturing these fungi. Each of the six isolates used in this study were crossed with each other, thereby producing a total of 15 potential mating combinations (Table B.13). Additionally, all isolates were also cultured in isolation to assess whether they were able to undergo unisexual reproduction. The cultures were incubated at 20 °C for a total of 21 days and were visually inspected for ascomatal production and maturation as well as ascospore exudation every 24-36 hours. Where mature ascomata and ascospores were produced, single ascospore masses were inoculated onto fresh MEA-ST plates and assessed for the production of ascomata, and thus the fertility of these spore masses, after seven days.

2.8.2 Growth rate

The growth rate of each knockout strain and all four wild type strains was assessed to determine whether the disruption of the *MAT1-2-7* gene had any effect on vegetative growth. This was achieved by excising 5 mm diameter mycelium-covered agar plugs and inoculating these onto sterile MEA-ST plates. Five plates of each isolate were used, and these cultures were grown for three days at 20 °C. Two measurements of colony diameter were taken perpendicular to each other at 60 hours post inoculation. The two measurements were averaged to produce a mean diameter of growth. The growth of each of the mutant strains was compared with that of the growth of the wild type isolates of both mating type using a two-tailed, independent t-test in Excel (v16.29).

2.9 RNA extraction, cDNA synthesis and RT-PCR

RNA was extracted from five-day-old, vegetatively-growing isolates including the two mutant strains as well as a MAT1 isolate (CMW 44436) and a MAT2 isolate (CMW

44442). RNA was also extracted from a five-day-old MAT1-1 (CMW 44436) x Δ *MAT127-H4* cross that produced protoascomata. These cultures were grown on MEA-ST overlaid with cellophane to allow for easy tissue harvesting. A total of three biological and three technical repeats were used, translating to nine MEA-ST plates of fungal tissue per isolate type.

Harvested tissue was flash frozen in liquid nitrogen and, using a sterile mortar and pestle, was ground into a fine powder. Total RNA was extracted using the RNeasy® Mini Kit (Qiagen, Limburg, The Netherlands) following the manufacturer's protocols. The RLC extraction buffer was used and the optional on-column DNase1 treatment was conducted. Gel electrophoresis (2% agarose gel, 120V, 25 min) was used to assess the integrity of the recovered RNA. The concentration of the RNA was estimated using an ND 1000 spectrophotometer (ThermoScientific, Waltham, USA).

The RNA was converted to cDNA using the RevertAid H Minus First Strand cDNA Synthesis Kit with oligo(dT)18 primers (ThermoScientific, Waltham, USA) to select for mRNA transcripts. In this synthesis reaction, 1 µg of total RNA, 0.5 mM primers and RNase-free water to a final volume of 5µl were combined and incubated for 5 minutes at 70°C, followed by incubation on ice for at least 5 minutes. This 5 µl reaction was then added to a solution containing 1X reaction buffer, $MgCl_2$ to a final concentration of 8mM, total dNTPs to a final concentration of 1 mM, 160 units of reverse transcriptase and RNase-free water to a final volume of 15 µl. The final 20 µl reaction was then incubated at 25°C for 5 minutes, 42°C for 1 hour and 70°C for 15 minutes. The resulting cDNA was diluted (1:20, 1:50, 1:100, 1:500, 1:1 000, 1:10 000, 1:100 000, 1:1 000 000 and 1:10 000 000) and subjected to PCR amplification using primers that targeted the two pheromone genes, the two pheromone receptors and *MAT1-2-1* (Fig. A.6, Table B.14). The dilution series of cDNA allowed for a semi-quantitative measurement of each of the genes' expression. RT-PCR amplification was conducted using a protocol that included a 5s/cycle extension of the annealing step and a total of 40 amplification cycles (Table B.14). Where possible, these primers were designed to flank introns to ensure that potential gDNA contamination could be identified if present. PCR products were visualized and purified as above. The PCR products were

also sequenced as described above to precisely confirm the predicted intron/exon boundaries and to determine if alternatively spliced transcripts of these genes were present.

3 RESULTS

3.1. sgRNA_2 successfully cleaves the *MAT1-2-7* target sequence *in vitro*

A total of 13 potential sgRNA molecules were predicted from the *H. omanensis MAT1-2-7* gene (Table B.15). A single construct, sgRNA_7, showed significant similarity to another region in the *H. omanensis* genome and was thus not considered in further analyses. Of the remaining 12 potential sgRNA molecules, four passed the RNA folding parameters, showing similar minimal free energy and centroid structures, with high binding probabilities. Finally, sgRNA_2 was chosen for further *in vitro* testing given that it targeted the most 5' region of the gene of the remaining sgRNA constructs (Fig. A.7).

The sgRNA_2 could support the efficient cleavage of the PCR product harbouring the target sequence. Gel electrophoresis revealed a significant length difference between the full-length PCR product (above 800 bp) and the cleaved product (above 700 bp). This sgRNA was thus used for the *in vivo* genome editing experiments.

3.2. Two knockout strains were isolated, *ΔMAT127-H1* and *ΔMAT127-H4*

A total of 26 isolates were capable of growing through the OCMA medium supplemented with 40 $ug.ml^{-1}$ hygromycin B. After transfer to MEA-50, 17 were capable of sustained growth and were thus considered successful transformants. PCR amplification and sequencing of the 5' and 3' integration sites showed that the dDNA had successfully integrated into the target region of two independent strains. Both integration events had resulted in the successful truncation of the *MAT1-2-7* gene (Fig. 3). These mutant strains, named *ΔMAT127-H1* and *ΔMAT127-H4*, showed exactly the same gene disruption pattern, harbouring the premature stop codon as well as the hygromycin resistance cassette at the region expected. In both cases, the stop codon

was introduced at nucleotide position 145 of the gene. Thus, if expressed, the gene would produce a protein product of only 48 aa, which is likely to be non-functional. Both isolates also showed stable integration of the hygromycin resistance cassette, as observed by the alternated transfers of these isolates from antibiotic-supplemented to unsupplemented media (Fig. A.8). Southern blot analysis confirmed the homologous integration of the hygromycin resistance cassette at a single region in the genome as well as the absence of heterologous integration of the cassette at other locations (Fig. A.8). Phenotypic analyses on both mutant strains showed very similar phenotypes.

3.3. *MAT1-2-7* disruption does not affect *MAT1-2-1* expression in *H. omanensis*

The *MAT* locus of many fungal species exhibits significant positional effects (Arnaise et al., 1997). Thus, any disruption to the *MAT* locus may have unexpected effects on the other genes present within this region and may lead to unintentional phenotypic effects. In an effort to ensure that the disruption of the *H. omanensis MAT1-2-7* did not affect *MAT1-2-1*, we assessed the expression of the *MAT1-2-1* gene via RT-PCR. The expression of *MAT1-2-1* was detected in vegetatively growing isolates of both mutant isolates as well the wild type MAT1-2 isolate- CMW 44442 (Fig. 4). The *MAT1-2-1* cDNA sequence of the mutant isolates was identical to that of the wild type MAT1-2 isolate. In all three isolates, the RNA had been fully processed and had undergone splicing to remove both introns. This indicated that the *MAT1-2-1* gene is expressed normally in the mutant strains and that any subsequent phenotypic differences were the result of *MAT1-2-7* disruption and not generalized *MAT* locus interference.

3.4. *MAT1-2-7* is essential for ascomatal development and maturation

Ascomatal development in *Huntiella* species (Fig. A.9) commences with the production of small, light-coloured, round protoascomata. This is followed by the emergence of a dark, beak-like structure from the young ascomatal base, which develops into an extended neck. During this process, the ascomatal base also darkens. Once mature, a sticky mass of ascospores is exuded from the tip of the neck.

In the crosses between MAT1-1 and MAT1-2 wild type isolates, mature ascomata were produced within 66 hours of co-inoculation and incubation at 20°C (Fig. 5). The ascomata consisted of dark, globose bases with extended necks (Fig. 5). A number of protoascomata were also seen at this stage in varying degrees of development; from light-coloured ascomatal bases with small beaks to darker bases with more pronounced immature necks. However, the majority of the ascomata were mature at this point. After approximately 90 hours, the ascomata began to exude ascospore masses from the tips of their necks. Ascospore masses that were transferred to sterile plates were capable of producing sexually-competent cultures within seven days (Fig. 5).

At 66 hours post co-inoculation, matings between a wild type MAT1-1 partner and either of the two mutant MAT1-2 partners had produced only immature protoascomata (Fig. 5). The majority of the ascomatal bases were light-coloured and only a few had begun to produce the dark, beak-like structures (Fig. 5). A similar phenotype was observed at 90 hours, with very little maturation of the immature ascomata. After 114 hours, the majority of the bases had darkened but the beaks had not developed into extended necks. By 21 days post-inoculation, the protoascomata had not matured beyond young, beaked structures, with the exception of the occasional structure with a short neck. No ascospores were produced by these protoascomata. When broken open, even the most mature of the protoascomata were devoid of any spore contents (Fig. 5).

We conducted a variety of control crosses between the two MAT1 isolates, the two MAT2 isolates and the two mutant isolates. We also paired each of the mutant isolates with each of the MAT2 isolates. Additionally, each of the six isolates were cultured in isolation. In all of these cases, no sexual development was observed.

3.5. Pheromone expression is altered in the mutant isolate

In *H. omanensis*, as is the case with other heterothallic species, MAT1-1 isolates almost exclusively express the α-pheromone and there is little to no expression of the **a**-pheromone. In contrast, MAT1-2 isolates express the **a**-pheromone, with little to no

expression of the α-pheromone (Wilson et al., 2018). The semi-quantitative PCR approach used in this study showed that the **a**-pheromone is expressed at high levels in the MAT1-2 wild type isolate, with detection of the **a**-pheromone mRNA transcript possible even in a 1:1 000 000 dilution. In contrast, the **a**-pheromone was expressed at lower levels in both the mutants, where transcripts were not detected at dilutions higher than 1:1 000 and 1:100 000 in the *ΔMAT127-H1* and *ΔMAT127-H4* isolates, respectively (Fig. 6). This suggested that the expression of the **a**-pheromone gene product is positively influenced by the MAT1-2-7 protein in *H. omanensis*. Thus, in the absence of a functional MAT1-2-7 gene product, there is less **a**-pheromone expression.

As expected, expression of the α-pheromone was detected in the wild type MAT1-1 isolate. In contrast, the expression of this gene was undetectable in the wild type MAT1-2 isolate (Fig. 7). The expression of this pheromone could also not be detected in the *ΔMAT127-H4* isolate. It was, however, possible to detect α-pheromone expression in the *ΔMAT127-H1* isolate. This indicated that while the disruption of the *MAT1-2-7* gene resulted in the negative regulation of the **a**-pheromone, it also up-regulated the α-pheromone, particularly in the *ΔMAT127-H1* isolate.

3.6. The pheromone receptors are alternatively spliced in *H. omanensis*

Different splice variants of the α- and **a**-pheromone receptors were expressed by isolates of both mating type (Fig. 8). In MAT1 isolates, the α-pheromone receptor was expressed with its intron unspliced, yielding a protein harbouring a premature stop codon and one that encodes only six of the seven transmembrane domains that characterize this type of receptor. It is unlikely that this form of the receptor protein would be functional, as the even number of transmembrane domains would preclude the existence of both intra- and extracellular domains. These MAT1 isolates also express the **a**-pheromone receptor, but in this case, the receptor's mRNA transcript is correctly spliced and thus produces a fully functional, seven-transmembrane domain protein. The reciprocal was true for MAT2 isolates, which produced a correctly spliced and presumably functional α-pheromone receptor with all seven transmembrane

domains, while the transcript of the **a**-pheromone receptor remained unspliced. This transcript would be translated into a protein harbouring only five transmembrane domains and was probably non-functional. The mutant isolates both expressed the pheromone receptors in the same manner as the wild type MAT2 isolate.

3.7. *MAT1-2-7* truncation does not lead to unisexuality in *H. omanensis*

The in-frame stop codon introduced into the *H. omanensis MAT1-2-7* gene closely mimicked that of the *H. moniliformis MAT1-2-7* gene, where the truncation is thought, in part, to be responsible for the unisexual phenotype observed in this species. However, *MAT1-2-7* disruption in *H. omanensis* did not result in this phenotype. Neither of the two mutant isolates were capable of protoascomatal development when cultured in isolation, which is the defining characteristic of unisexual reproduction in filamentous ascomycetes. Furthermore, crosses between the mutant isolates and the MAT1-2 did not result in the production of either protoascomata or ascomata.

3.8. *MAT1-2-7* is involved in vegetative growth

The average radial growth rate of the mutant isolates was significantly slower than that of the wild type isolates of both mating types (Fig. 9, Tables B.16 – B.17). By the 60-hour time point, all four wild type isolates grew to an average diameter of up to 59 mm, while both mutants strains had average diameters of up to 41 mm in the same period. The culture morphology of the mutants was also different to that of the wild type. While wild type isolates of both mating types formed aerial hyphae with a “fluffy” phenotype, both mutants produced much smoother mycelia that was submerged within in the agar (Fig. 9).

4 DISCUSSION

The development of an efficient and effective transformation and genome editing protocol for use in *Huntiella* species has been a valuable addition to the molecular toolkit available for these species. This protocol will finally allow for the functional characterization of genes involved in many biological processes, such as sexual reproduction, growth and host-

specificity. Furthermore, it will likely be possible to extend the methods used here to some of the other economically relevant species that reside in the Ceratocystidaceae. In this study, this technique was used to functionally characterize the novel *H. omanensis* mating gene, *MAT1-2-7*, with regards to its role in sexual reproduction. We disrupted the gene by introducing an in-frame stop codon at a position that mimicked the truncation seen in the *H. moniliformis MAT1-2-7* gene. We were thus able to show that *MAT1-2-7* is a true mating gene that is essential for sexual reproduction. Furthermore, we also showed that it exhibited pleiotropic effects by influencing radial growth rate in this fungus.

This study showed that *MAT1-2-7* was essential for ascomatal maturation in *H. omanensis*, a process that has been closely linked with the secondary *MAT* genes of other ascomycete species as well (Arnaise et al., 1997; Kim et al., 2012; Yu et al., 2017). Crosses between wild type MAT1-1 and MAT1-2 isolates of *H. omanensis* produced mature, ascospore-exuding ascomata within four days of co-incubation (Wilson et al., 2015). Transfer of the ascospore masses could produce sexually reproducing cultures within a further seven days. However, crosses between a wild type MAT1-1 isolate of *H. omanensis* and either of the two *⊿MAT1-2-7* mutant isolates produced only protoascomata at the zone of interaction. The development of these structures was delayed compared to that of the wild type crosses, and they never developed to maturity. Furthermore, no ascospores were produced in these sexual structures, suggesting that the production of sexual spores is entirely precluded in these mutant isolates, even in the presence of a wild type mating partner.

Given that protoascomatal maturation occurs fairly early during the process of mating, it appears that the *H. omanensis MAT1-2-7* is important during the initial phases of sexual reproduction. Interestingly, the *H. omanensis MAT1-2-7* truncation resulted in a phenotype comparable to that of other species in which secondary *MAT* genes have also been disturbed. The disruption of the *Podospora anserina MAT1-1-2* (Arnaise et al., 2001, 1997), the *Fusarium graminearum MAT1-1-2* and *MAT1-1-3* (Kim et al., 2012), the *Sordaria macrospora MAT1-1-2* (Klix et al., 2010), the *Botrytis MAT1-1-5* and *MAT1-2-10* (Rodenburg et al., 2018) and *Aspergillus fumigatus MAT1-2-4* (Yu et al., 2017), resulted in the production of immature protoascomata that never develop or fully mature, but barren, ascomata. These results support the notion that a finer control of sexual reproduction has been

achieved by the acquisition of secondary *MAT* genes (Yu et al., 2017). Thus, instead of being responsible for sexual initiation, as is the role of the primary *MAT* genes (Kim et al., 2012; Rodenburg et al., 2018), they are instead important for further development.

In ascomycete fungi, one of the direct targets of the MAT transcription factors is the pheromone response pathway (Bobrowicz et al., 2002; Shen et al., 1999; Zhang et al., 1998). In particular, the pheromone genes are typically transcriptionally controlled by the proteins encoded by the *MAT* locus. It is thus likely that the underlying mechanism by which *MAT1-2-7* disruption affects ascomatal development is via the pheromone response pathway. This is supported by the fact that both of the *ΔMAT1-2-7* mutants showed a decrease in the expression of the **a**-pheromone, the mating pheromone usually expressed by MAT2 isolates. Furthermore, one of the two mutants was able to express the α-pheromone, suggesting that the normal mating-type dependent regulation of the pheromones in *H. omanensis* (Wilson et al., 2018) has been affected by the *MAT1-2-7* knockout. In other filamentous ascomycete fungi, such as *P. anserina* (Coppin et al., 2004) and *N. crassa* (Kim and Borkovich, 2006), the expression of the mating pheromones is closely linked with male fertility. In these species, the downregulation or complete knockout of the pheromone-encoding genes results in isolates that are female fertile, but unable to produce the male cells that are capable of fertilizing the female structures of an opposite mating type. Given the downregulation of the **a**-pheromone in the MAT1-2 isolates harbouring the disrupted *MAT1-2-7* gene, it is possible that the maturation of protoascomata is precluded by an inability of the MAT1-2 isolate to fertilize the female structures of the MAT1-1 partner.

Significant differences are apparent in the phenotypes of the artificially introduced and naturally occurring *MAT1-2-7* truncations, as seen in *H. omanensis* and *H. moniliformis*, respectively. In *H. moniliforms*, sexual reproduction is not precluded, and instead, MAT1-2 isolates of this species are capable of sexual reproduction even in the absence of a MAT1-1 mating partner (Wilson et al., 2018, 2015). In contrast, the truncation in *H. omanensis* leads to a complete halt in ascomatal development even in the presence of a wild type mating partner. This suggests that while the disruption of the *MAT1-2-7* gene in *H. moniliformis* may have played a role in the evolution towards unisexuality, this change alone was not sufficient to shift its reproductive strategy. In fact, the indiscriminate expression of both

pheromone types in *H. moniliformis* has also been hypothesized to play a role in the ability of this species to unisexually reproduce (Wilson et al., 2018). Interestingly, one of the two *H. omanensis* mutant strains was capable of expressing both the **a**- and α-pheromone types and yet was incapable of unisexual reproduction. This suggests that there are other, yet to be investigated, genes that are also involved in the unisexual pathway or that the isolate is unable to recognize the endogenously produced pheromones.

Despite the fact that the mutant isolates harbour an identical *MAT1-2-7* gene disruption, there are significant differences between the pheromone expression patterns of the two isolates. Most notable is the absence of detectable α-pheromone expression in the *ΔMAT127-H4* mutant, despite the expression of this pheromone in the *ΔMAT127-H1* mutant. One potential explanation for this is sensitivity of the *MAT* locus to genetic manipulation (Arnaise et al., 1997, Yu et al., 2017). Although the final product, in the form of *MAT1-2-7* truncation, is identical in both isolates, the physical DNA breakage and repair that occurred during editing may have been different between the two isolates- perhaps in efficiency or accuracy. This could have caused a form of *MAT* locus disruption that could not be detected in this study. Given the importance of the physical location of the *MAT* genes (Arnaise et al., 1997, Yu et al., 2017) and their importance in the regulation of the pheromone genes, it is possible that generalized *MAT* locus disruption could have varying effects on the ability of the locus to control mating. Alternatively, although every effort was made to ensure that we limited the potential for off-target effects, it is possible that the genome of one of the mutant isolates has been edited in a region outside of the *MAT* locus. Whole genome sequencing will be conducted in the future in order to assess both of these possibilities.

A final factor that could contribute to the lack of unisexual reproduction in the two mutant *H. omanensis* isolates is the mating-type specific alternative splicing of the pheromone receptor genes. In most ascomycete species, both MAT1-1 and MAT1-2 isolates express both pheromone receptors and thus mating specificity is mediated solely by the mating-type dependent expression of the pheromones (Pöggeler and Kück, 2001). In this study, we showed that *H. omanensis* isolates express both receptors but only produce functional versions of the receptor with which they will recognize an opposite mating partner. Thus,

MAT2 isolates, which express the **a**-pheromone and recognize the α-pheromone, only express a functional α-pheromone receptor. This was also true of the two mutant isolates. Thus, although the mutants do express the **a**-pheromone, they are potentially unable to produce a functional **a**-pheromone receptor with which to recognize and respond to the pheromone. Of course, one of the mutant isolates was capable of α-pheromone expression and also a functional version of the α-pheromone receptor. It is thus possible that unisexual reproduction relies on the expression and recognition of both pheromones. It would be interesting to determine whether similar alternative splicing events occur in the pheromone receptors of *H. moniliformis*.

To the best of our knowledge, this is the first report of alternative splicing being used to potentially aid in partner recognition via the pheromone receptors. This may have evolved as a mechanism to promote outcrossing in a system where indiscriminate pheromone expression was possible and both pheromones are produced by a single individual (Wilson et al., 2018). Thus, instead of relying solely on mating type dependent pheromone expression as a barrier to inbreeding, mating type specific alternative splicing of the pheromone receptors also ensure that only MAT1-1 and MAT1-2 partners can recognize each other as suitable partners.

Despite being primarily involved in mating, certain *MAT* genes can exhibit pleiotropic effects, affecting processes such as growth (Lee et al., 2015), virulence (Lee et al., 2015) and vegetative incompatibility (Newmeyer et al., 1973). This is certainly the case for the *H. omanensis*, where vegetative growth was significantly affected in both of the *ΔMAT1-2-7* mutant isolates. While wild type *H. omanensis* isolates of both mating types grow rapidly and produce aerial mycelia, the mutant strains grew submerged within the agar and more slowly. A similar phenotype is seen in *Ceratocystis albifundus*, where deletion of *MAT1-2-1* during mating type switching has a direct effect on the growth of these isolates (Lee et al., 2015). It may not be surprising that sexual reproduction and vegetative growth were linked, as both are intimately linked to secondary metabolism and the regulation of the associated biochemical pathways (Calvo et al., 2002). The underlying mechanism of these pleiotropic effects remains unknown and will need to be investigated in the future.

This study is the first to successfully genetically manipulate any species of *Huntiella*, providing a convenient system with which to functionally characterize the novel *MAT1-2-7* gene. Genetic manipulation was achieved by developing a protoplast-based transformation protocol established on those established in other filamentous fungi (Chung and Lee, 2015; Leung et al., 1990). This was combined with a fairly novel use of the CRISPR-Cas9 genome editing system in fungi, whereby the sgRNA and a purified Cas9 enzyme were combined *in vitro* to form the RNP before being used for transformation *in vivo*. This method allowed us to overcome certain challenges associated with the classical plasmid-based CRISPR-Cas9 system (Nagy et al., 2017; Wang et al., 2018), such as sufficient Cas9 expression and potentially random genomic integration. A similar technique was recently used in *F. oxysporum* (Wang et al., 2018) and *Mucor circinelloides* (Nagy et al., 2017) and we thus propose that this method will allow for successful gene characterization in other non-model species for which the molecular toolkit is still limited.

5 CONCLUSION

This study is the first to report the successful genetic manipulation of any species of *Huntiella*. It thus represents a valuable addition to molecular toolkit that is available to thoroughly investigate the biology of these species. This study focused on ascertaining the function of *MAT1-2-7* in the sexual cycle of *H. omanensis*, but the functions of genes involved in other biological processes like asexual reproduction, growth and host-specificity can now be better interrogated and underlying genetic mechanisms can be elucidated. Furthermore, this protocol can be used as a base from which species-specific protocol optimization can be conducted, allowing for the development of a similar protocol in the other, economically important species residing in the Ceratocystidaceae.

6 ACKNOWLEDGEMENTS

We would like to thank Mr Matthew Weatley and Prof Yinong Yang, both of whom provided invaluable insight into the CRISPR-Cas9 system developed for this study. Further experimental support was received from both Dr Tuan Duong and Ms Mmatshepho Phasha.

We would also like to thank Prof Cobus Visagie for producing a number of the photographic and micrographic images included in this study.

7 FUNDING

This project was supported by the University of Pretoria, the Department of Science and Technology (DST)/National Research Foundation (NRF) Centre of Excellence in Tree Health Biotechnology (CTHB). The project was additionally supported by Prof BD Wingfield's DST/NRF SARCHi chair in Fungal Genomics (Grant number: 98353). The grant holders acknowledge that opinions, findings and conclusions or recommendations expressed in this piece of work are that of the researchers and that the funding bodies accept no liability whatsoever in this regard.

8 REFERENCES

Arnaise, S., Debuchy, R., Picard, M., 1997. What is a *bona fide* mating-type gene? Internuclear complementation of *mat* mutants in *Podospora anserina*. Mol. Gen. Genet. 256, 169–178. https://doi.org/10.1007/PL00008611

Arnaise, S., Zickler, D., Le Bilcot, S., Poisier, C., Debuchy, R., 2001. Mutations in mating-type genes of the heterothallic fungus *Podospora anserina* lead to self-fertility. Genetics 159, 545–556.

Bobrowicz, P., Pawlak, R., Correa, A., Bell-Pedersen, D., Ebbole, D.J., 2002. The *Neurospora crassa* pheromone precursor genes are regulated by the mating type locus and the circadian clock. Mol. Microbiol. 45, 795–804. https://doi.org/10.1046/j.1365-2958.2002.03052.x

Calvo, A.M., Wilson, R.A., Bok, J.W., Keller, N.P., 2002. Relationship between secondary metabolism and fungal development. Microbiol. Mol. Biol. Rev. 66, 447–459. https://doi.org/10.1128/MMBR.66.3.447

Carroll, A.M., Sweigard, J.A., Valent, B., 1994. Improved vectors for selecting resistance to hygromycin. Fungal Genet. Rep. 41, 41–44.

Chung, K.-R., Lee, M.-H., 2015. Split-marker-mediated transformation and targeted gene disruption in filamentous fungi, in: van den Berg, M.A., Maruthachalam, K. (Eds.), Genetic Transformation Systems in Fungi. Springer International Publishing, Cham, pp.

175–180. https://doi.org/10.1007/978-3-319-10503-1_15

Coppin, E., de Renty, C., Debuchy, R., 2004. The function of the coding sequences for the putative pheromone precursors in *Podospora anserina* is restricted to fertilization. Eukaryot. Cell 4, 407–420. https://doi.org/10.1128/ec.4.2.407-420.2005

de Beer, Z.W., Duong, T.A., Barnes, I., Wingfield, B.D., Wingfield, M.J., 2014. Redefining *Ceratocystis* and allied genera. Stud. Mycol. 79, 187–219. https://doi.org/10.1016/j.simyco.2014.10.001

Debuchy, R., Berteaux-Lecellier, V., Silar, P., 2010. Mating systems and sexual morphogenesis in ascomycetes, in: Borkovich, K.A., Ebbole, D.J. (Eds.), Cellular and Molecular Biology of Filamentous Fungi. ASM Press, Washington D.C., pp. 501–535. https://doi.org/10.1128/9781555816636.ch33

Debuchy, R., Coppin, E., 1992. The mating types of *Podospora anserina*: Functional analysis and sequence of the fertilization domains. Mol. Gen. Genet. 233, 113–121. https://doi.org/10.1007/BF00587568

Dyer, P.S., Inderbitzin, P., Debuchy, R., 2016. Mating-type structure, function, regulation and evolution in the Pezizomycotina, in: Growth, Differentiation and Sexuality. Springer International Publishing, pp. 351–385. https://doi.org/10.1007/978-3-319-25844-7_14

Eisel, D., Seth, O., Grunewald-Janho, S., Krunchen, D., Ruger, B., 2008. DIG application manual: For filter hybridization. Roche Diagnostics.

Ferreira, A.V.B., An, Z., Metzenberg, R.L., Glass, N.L., 1998. Characterization of *mat A-2*, *mat A-3* and *ΔmatA* mating-type mutants of *Neurospora crassa*. Genetics 148, 1069–1079.

Gasiunas, G., Barrangou, R., Horvath, P., Siksnys, V., 2012. Cas9–crRNA ribonucleoprotein complex mediates specific DNA cleavage for adaptive immunity in bacteria. Proc. Natl. Acad. Sci. 109, 2579–2586. https://doi.org/10.1073/pnas.1208507109

Gruber, A.R., Lorenz, R., Bernhart, S.H., Neubo, R., Hofacker, I.L., 2008. The Vienna RNA websuite. Nucleic Acids Res. 36, W70–W74. https://doi.org/10.1093/nar/gkn188

Jinek, M., Chylinski, K., Fonfara, I., Hauer, M., Doudna, J.A., Charpentier, E., 2012. A programmable dual-RNA-guided DNA endonuclease in adaptive bacterial immunity. Science (80-.). 337, 816–822.

Kim, H., Borkovich, K.A., 2006. Pheromones are essential for male fertility and sufficient to direct chemotropic polarized growth of trichogynes during mating in *Neurospora crassa*. Eukaryot. Cell 5, 544–554. https://doi.org/10.1128/ec.5.3.544-554.2006

Kim, H.K., Cho, E.J., Lee, S., Lee, Y.S., Yun, S.H., 2012. Functional analyses of individual mating-type transcripts at *MAT* loci in *Fusarium graminearum* and *Fusarium asiaticum*. FEMS Microbiol. Lett. 337, 89–96. https://doi.org/10.1111/1574-6968.12012

Klix, V., Nowrousian, M., Ringelberg, C., Loros, J.J., Dunlap, J.C., Pöggeler, S., 2010. Functional characterization of *MAT1-1*-specific mating-type genes in the homothallic ascomycete *Sordaria macrospora* provides new insights into essential and nonessential sexual regulators. Eukaryot. Cell 9, 894–905. https://doi.org/10.1128/ec.00019-10

Lee, D.H., Roux, J., Wingfield, B.D., Wingfield, M.J., 2015. Variation in growth rates and aggressiveness of naturally occurring self-fertile and self-sterile isolates of the wilt pathogen *Ceratocystis albifundus*. Plant Pathol. 64, 1103–1109. https://doi.org/10.1111/ppa.12349

Leung, H., Lehtinen, U., Karjalainen, R., Skinner, D., Tooley, P., Leong, S., Ellingboe, A., 1990. Transformation of the rest blast fungus *Magnaporte grisea* to hygromycin B resistance. Curr. Genet. 17, 409–411.

Martin, S.H., Wingfield, B.D., Wingfield, M.J., Steenkamp, E.T., 2011. Structure and evolution of the *Fusarium* mating type locus: New insights from the *Gibberella fujikuroi* complex. Fungal Genet. Biol. 48, 731–740. https://doi.org/10.1016/j.fgb.2011.03.005

McGuire, I.C., Marra, R.E., Turgeon, B.G., Milgroom, M.G., 2001. Analysis of mating-type genes in the chestnut blight fungus, *Cryphonectria parasitica*. Fungal Genet. Biol. 34, 131–144. https://doi.org/10.1006/fgbi.2001.1295

Nagy, G., Szebenyi, C., Csernetics, Á., Vaz, A.G., Judit, E., Vágvölgyi, C., Papp, T., 2017. Development of a plasmid free CRISPR-Cas9 system for the genetic modification of *Mucor circinelloides*. Sci. Rep. 7, 1–10. https://doi.org/10.1038/s41598-017-17118-2

Newmeyer, D., Branch Howe, H., Galeazzi, D., 1973. A search for complexity at the mating-type locus of *Neurospora crassa*. Can. J. Genet. Cytol. 15, 577–585.

Paoletti, M., Seymour, F.A., Alcocer, M.J.C., Kaur, N., Calvo, A.M., Archer, D.B., Dyer, P.S., 2007. Mating type and the genetic basis of self-fertility in the model fungus *Aspergillus nidulans*. Curr. Biol. 17, 1384–1389. https://doi.org/10.1016/j.cub.2007.07.012

Pöggeler, S., Kück, U., 2001. Identification of transcriptionally expressed pheromone receptor genes in filamentous ascomycetes. Gene 280, 9–17. https://doi.org/10.1016/S0378-1119(01)00786-7

Pöggeler, S., Kück, U., 2000. Comparative analysis of the mating-type loci from *Neurospora*

crassa and *Sordaria macrospora*: Identification of novel transcribed ORFs. Mol. Gen. Genet. 263, 292–301. https://doi.org/10.1007/s004380051171

Ran, F.A., Hsu, P.D., Wright, J., Agarwala, V., Scott, D.A., Zhang, F., 2013. Genome engineering using the CRISPR-Cas9 system. Cell 8, 2281–2308. https://doi.org/10.1038/nprot.2013.143

Rodenburg, S.Y.A., Terhem, R.B., Veloso, J., Stassen, J.H.M., van Kan, J.A.L., 2018. Functional analysis of mating type genes and transcriptome analysis during fruiting body development of *Botrytis cinerea*. MBio 9, 1–19. https://doi.org/10.1128/mbio.01939-17

Sambrook, J., Green, M., 2012. Molecular cloning: A laboratory manual, 4th ed. Cold Spring Harbor Laboratory Press.

Shen, W.C., Bobrowicz, P., Ebbole, D.J., 1999. Isolation of pheromone precursor genes of *Magnaporthe grisea*. Fungal Genet. Biol. 27, 253–263. https://doi.org/10.1006/fgbi.1999.1151

Staben, C., Yanofsky, C., 1990. *Neurospora crassa* a mating-type region. Genetics 87, 4917–4921.

Turgeon, B.G., Yoder, O.C., 2000. Proposed nomenclature for mating type genes of filamentous ascomycetes. Fungal Genet. Biol. 31, 1–5. https://doi.org/10.1006/fgbi.2000.1227

Wang, Q., Cobine, P.A., Coleman, J.J., 2018. Efficient genome editing in Fusarium oxysporum based on CRISPR/Cas9 ribonucleoprotein complexes. Fungal Genet. Biol. 117, 21–29. https://doi.org/10.1016/j.fgb.2018.05.003

Wilken, P.M., Steenkamp, E.T., Wingfield, M.J., de Beer, Z.W., Wingfield, B.D., 2017. Which *MAT* gene? Pezizomycotina (Ascomycota) mating-type gene nomenclature reconsidered. Fungal Biol. Rev. 31, 199–211. https://doi.org/10.1016/j.fbr.2017.05.003

Wilson, A.M., Godlonton, T., van der Nest, M.A., Wilken, P.M., Wingfield, M.J., Wingfield, B.D., 2015. Unisexual reproduction in *Huntiella moniliformis*. Fungal Genet. Biol. 80, 1–9. https://doi.org/10.1016/j.fgb.2015.04.008

Wilson, A.M., van der Nest, M.A., Wilken, P.M., Wingfield, M.J., Wingfield, B.D., 2018. Pheromone expression reveals putative mechanism of unisexuality in a saprobic ascomycete fungus. PLoS One 13, e0192517. https://doi.org/10.1371/journal.pone.0192517

Yu, Y., Amich, J., Will, C., Eagle, C.E., Dyer, P.S., Krappmann, S., 2017. The novel *Aspergillus fumigatus MAT1-2-4* mating-type gene is required for mating and cleistothecia formation. Fungal Genet. Biol. 108, 1–12. https://doi.org/10.1016/j.fgb.2017.09.001

Zhang, L., Baasiri, R.A., Van Alfen, N.K., 1998. Viral repression of fungal pheromone precursor gene expression. Mol. Cell. Biol. 18, 953–959. https://doi.org/10.1128/mcb.18.2.953

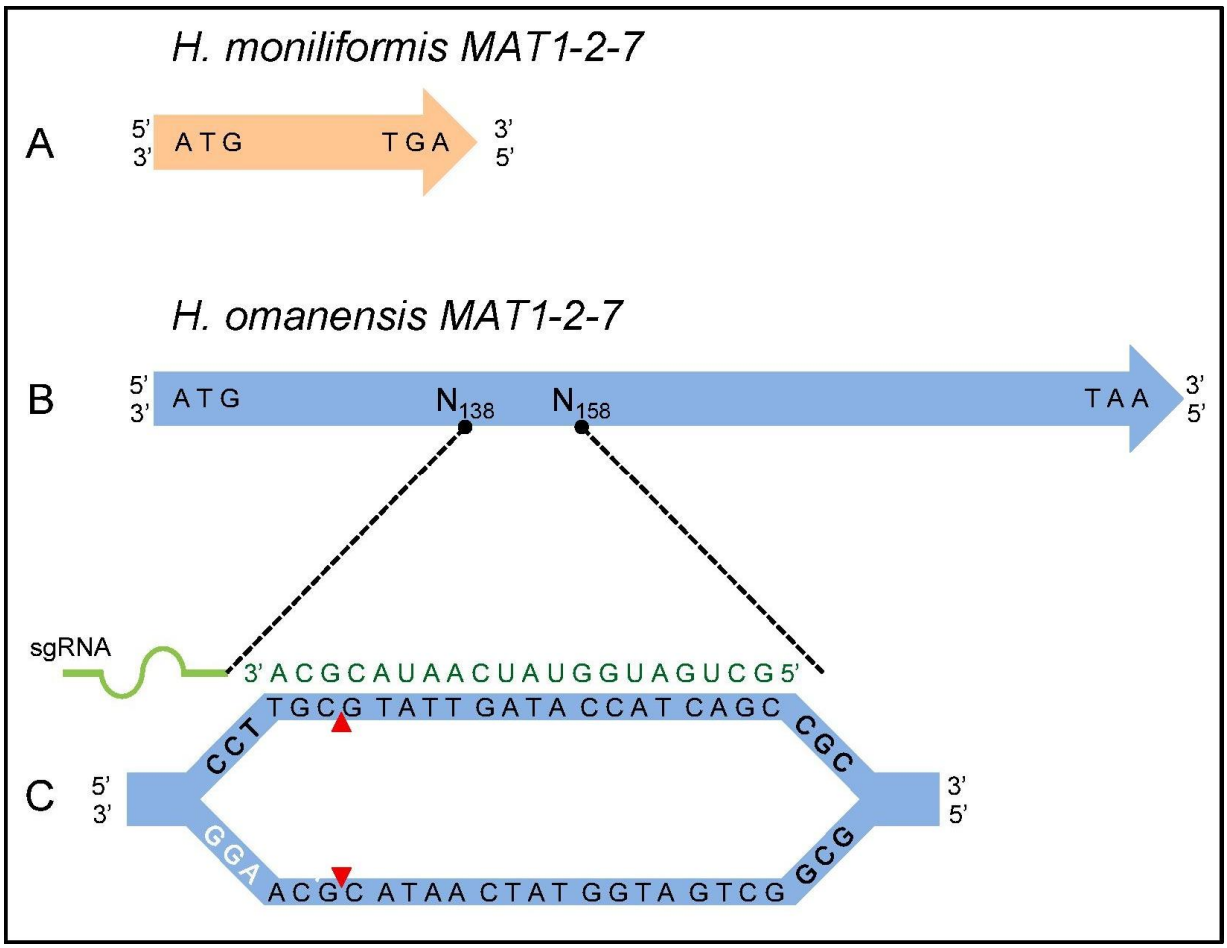

Fig. 1. The design of the sgRNA. The sgRNA was designed in such a way to ensure that the knockout of the *H. omanensis MAT1-2-7* gene resulted in gene truncation similar to that of *H. moniliformis*. The designed sgRNA targets the N_{138} to N_{158} region of the *H. omanensis MAT1-2-7* gene as it is in this region that the premature stop codon is found in the *H. moniliformis MAT1-2-7*. (A) The *H. moniliformis MAT1-2-7* gene is only 147 nt in length and thus less than a third of (B) the *H. omanensis MAT1-2-7* gene, which is 468 nt in length. (C) Illustration of the sgRNA target region. The scaffold of the sgRNA is indicated in light green with the protospacer sequence indicated by the adjacent green nucleotides. The PAM sequence is indicated as white text on the bottom strand. The predicted Cas9 cut site is indicated by the red arrows.

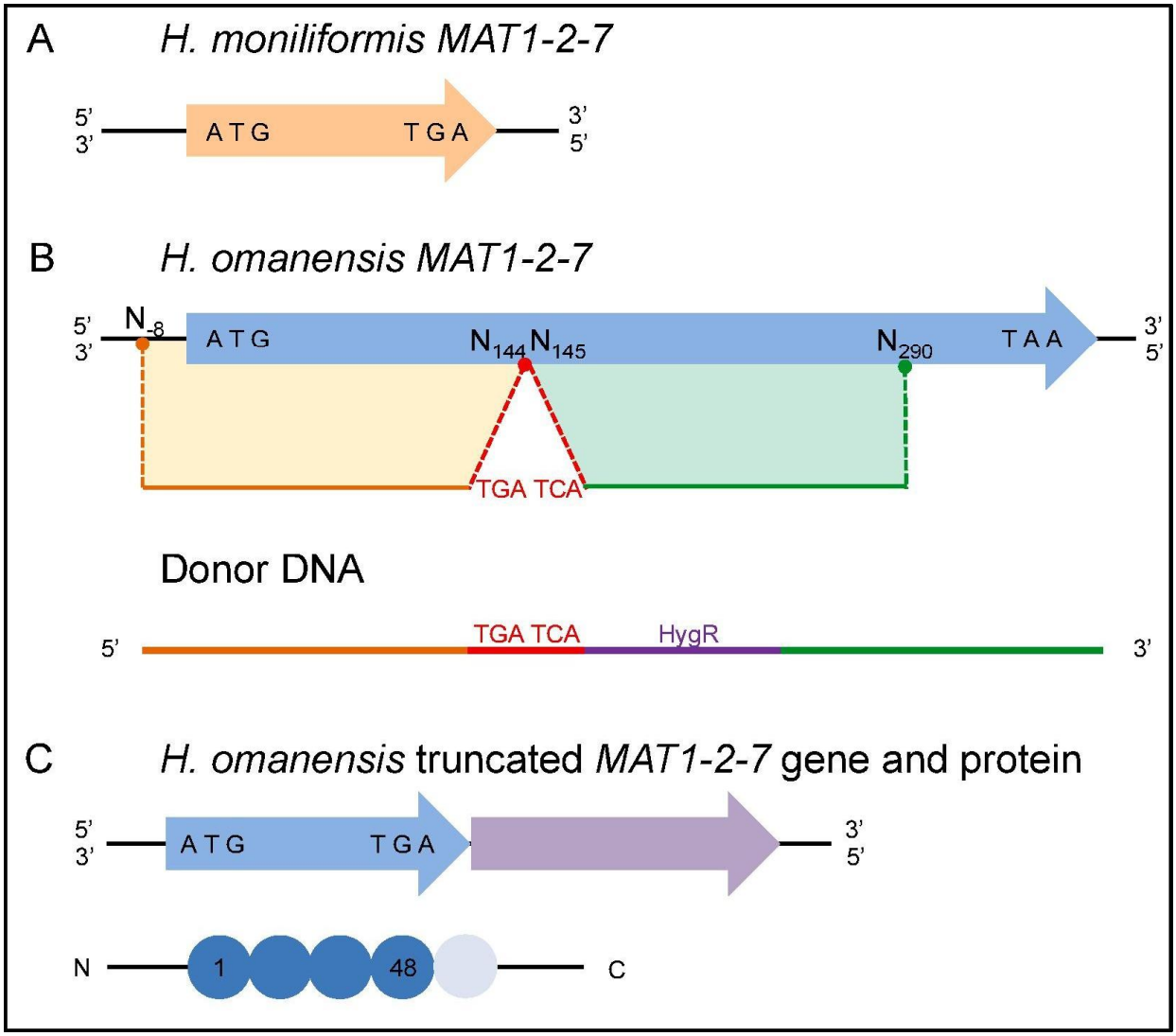

Fig. 2. Designing the donor DNA. The dDNA, similar to the sgRNA, was designed to ensure that the knockout of the *H. omanensis MAT1-2-7* gene resulted in gene truncation similar to that seen in *H. moniliformis*. (A) The premature stop codon (TGA) found in the *H. moniliformis MAT1-2-7* gene is at nucleotide positions N_{145} – N_{147} and codon position C_{49}. (B) The donor DNA has been designed to including the *BSII* restriction enzyme (RE) cut site (red) and the hygromycin B resistance cassette (purple), flanked by regions of homology (orange and green) to the genomic region harbouring the *MAT1-2-7*. The RE site was designed to occur in frame with the *MAT1-2-7* coding sequence and thus introduces the stop codon, TGA, leading to the premature termination of translation. (C) After Cas9-mediated cutting and homologous recombination of the dDNA, the *H. omanensis MAT1-2-7* gene possessed a premature stop codon which would result in the translation of a 48 aa protein. The gene models are not drawn to scale.

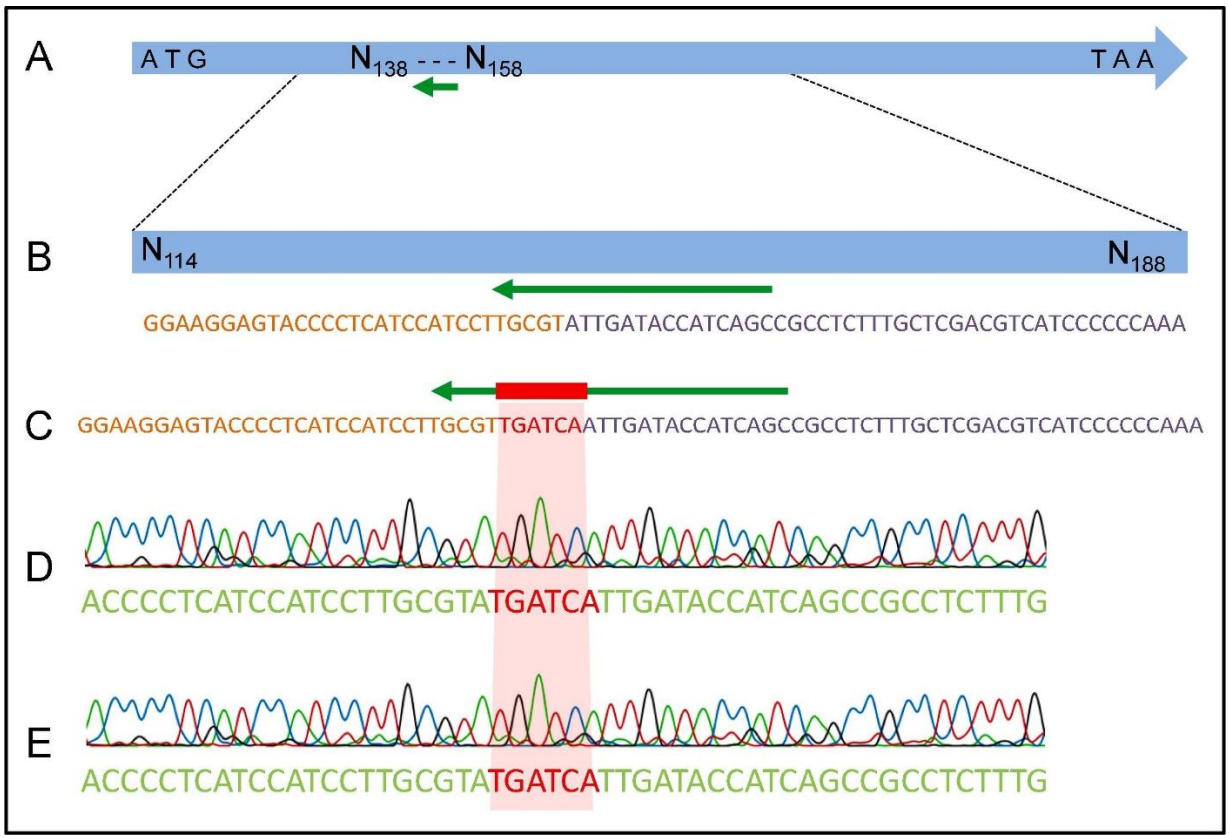

Fig. 3. The successful integration of the *BclI* restriction enzyme site, including the TGA stop codon, into the *MAT1-2* idiomorph of *H. omanensis*. (A) The full-length *H. omanensis MAT1-2-7* gene, with the sgRNA target site indicated by the green arrow between nucleotides 138 and 158. (B) A magnified schematic of the sgRNA target site within the *H. omanensis MAT1-2-7* gene. (C) A magnified schematic of a region of the dDNA showing the *BclI* RE site flanked by arms homologous to the *MAT1-2* locus of *H. omanensis*. (D and E) Sanger sequence chromatogram indicating the successful integration of the *BclI* RE site into the *MAT1-2-7* gene of isolates *ΔMAT127-H1* and *ΔMAT127-H4*, respectively.

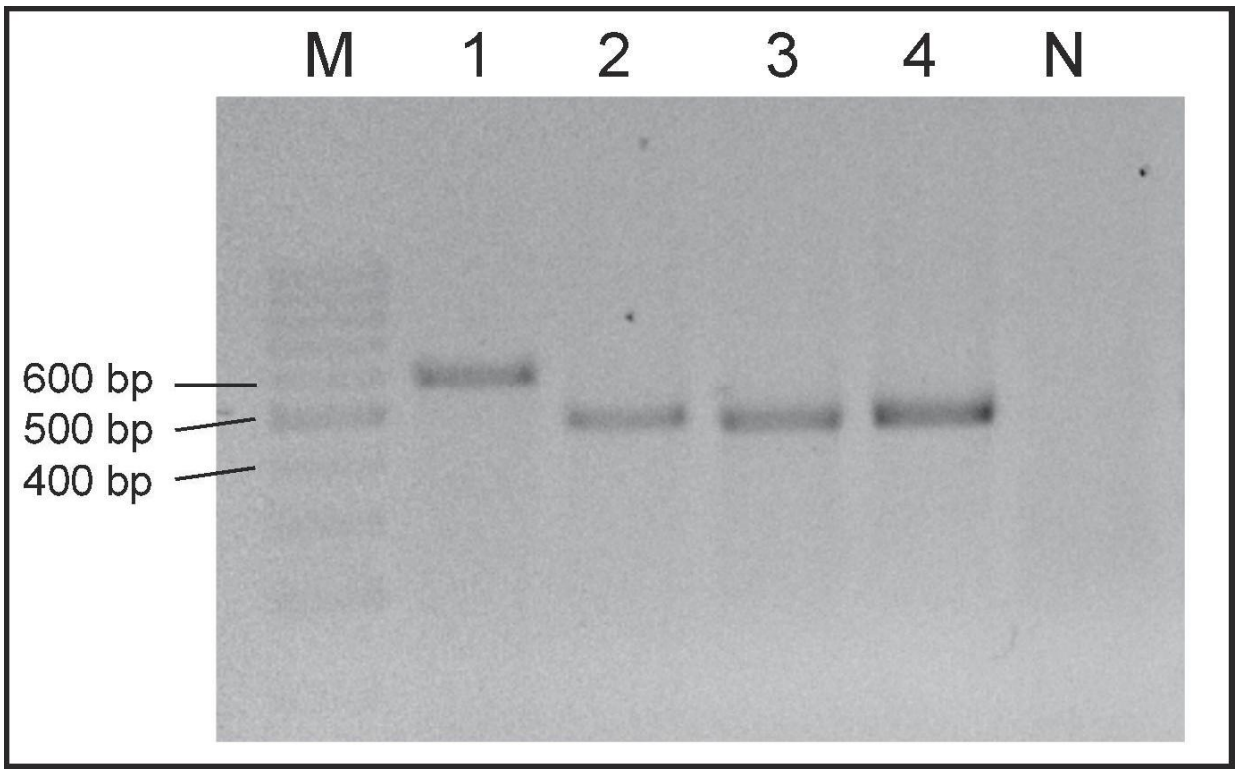

Fig. 4. Expression and splicing of the *H. omanensis MAT1-2-1*. The *MAT1-2-1* gene of *H. omanensis* has a single intron of 53 nt which is spliced out after transcription. Lane 1 shows a *MAT1-2-1* PCR product derived from the gDNA of a MAT1-2 wildtype isolate (CMW 44442). Lanes 2 – 4 show the *MAT1-2-1* PCR products produced from the cDNA of a MAT1-2 wild type isolate (CMW 44442), and cDNA from the two mutant isolates, *ΔMAT127-H1* (CMW 54810) and *ΔMAT127-H4* (CMW 54811). The mutant isolates express the *MAT1-2-1* gene as expected and also correctly splice out the intron before translation- suggesting that the *MAT1-2-1* gene is unaffected by the disruption of the *MAT1-2-7* gene. Lanes M and N show the 100 bp molecular marker and negative control, respectively.

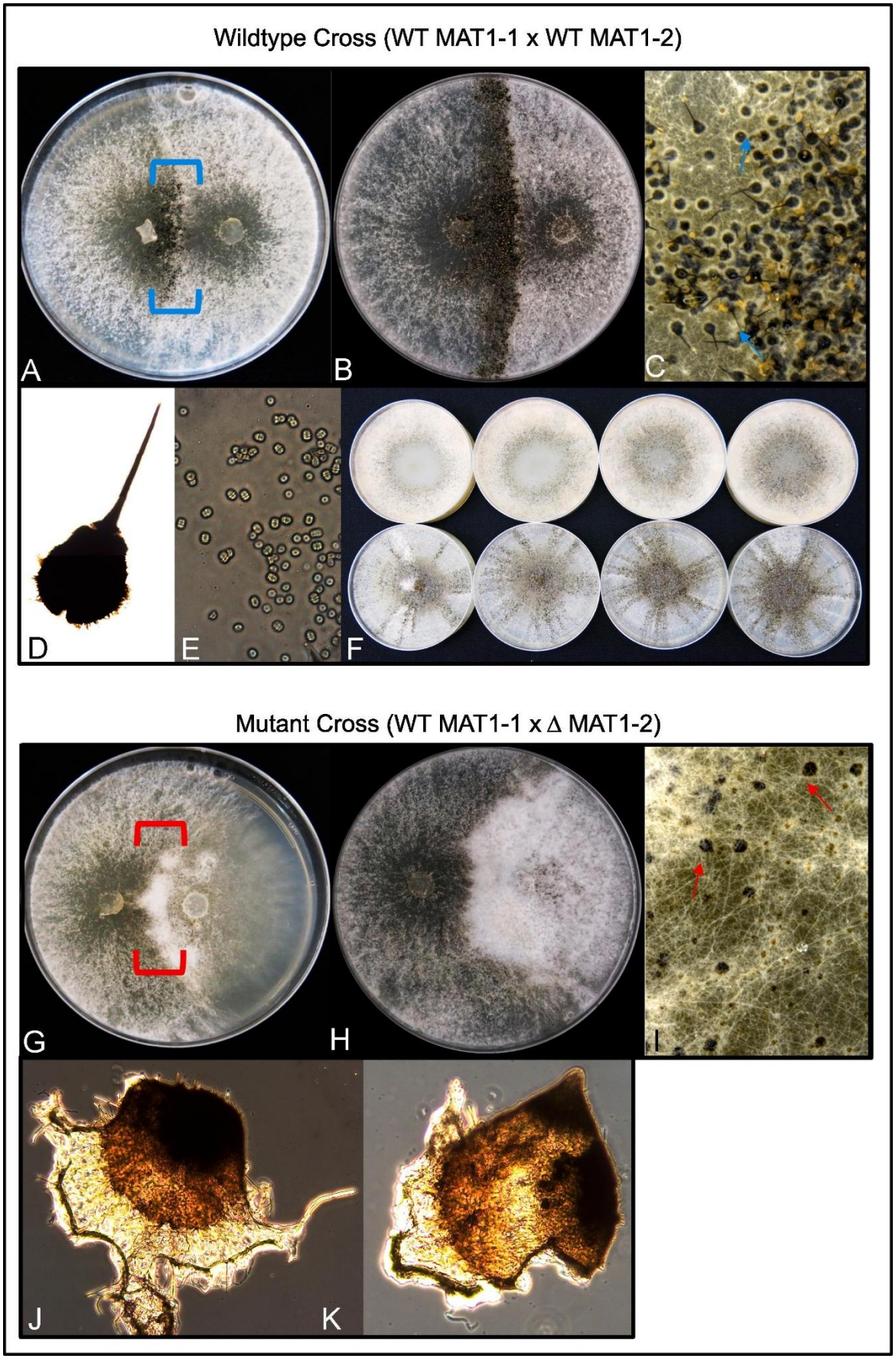
Wildtype Cross (WT MAT1-1 x WT MAT1-2)
A
B
C
D
E
F
Mutant Cross (WT MAT1-1 x Δ MAT1-2)
G
H
I
J
K

Fig. 5. Sexual development in matings between wildtype isolates (top panel) and between a MAT1-1 wildtype isolate and a MAT1-2 mutant isolate (bottom panel). (A) In the wildtype matings, sexual development is observed as early as 66 hours post co-incubation, where mature ascomata can be observed at the zone of interaction (indicated in blue). (B) At 90 hours post co-incubation, the wildtype crosses had produced ascospore masses which had exuded from the tips of the mature ascomatal necks. (C) At this timepoint, the wildtype crosses produced fully mature, ascospore-bearing ascomata (particularly clear examples indicated by the blue arrows). (D) A mature ascomata, a dark globose base and an extended neck, characteristics of *Huntiella* species. The hat-shaped ascospores, pictured in (E) exuded from the pore found at the top of the ascomatal neck. (F) The sexually competent cultures produced by transferring ascospore masses from the wildtype cross onto sterile plates. (G) At 66 hours post co-incubation of the matings including a MAT1-2 mutant isolate, only immature protoascomata had been formed in the zone of interaction (indicated in red). (H) At 90 hours post co-incubation, these protoascomata had only slightly matured, with most harbouring small darkened beaks. (I) At this timepoint, the most mature sexual structures observed in these crosses were dark and slightly beaked protoascomata (particularly clear examples indicated by the red arrows). (J) A young protoascomata beginning to darken. (K) The most mature sexual structure formed in the mutant cross: a maturing protoascomata exhibiting the beak-like structure which, in wildtype crosses, would have extended into the neck.

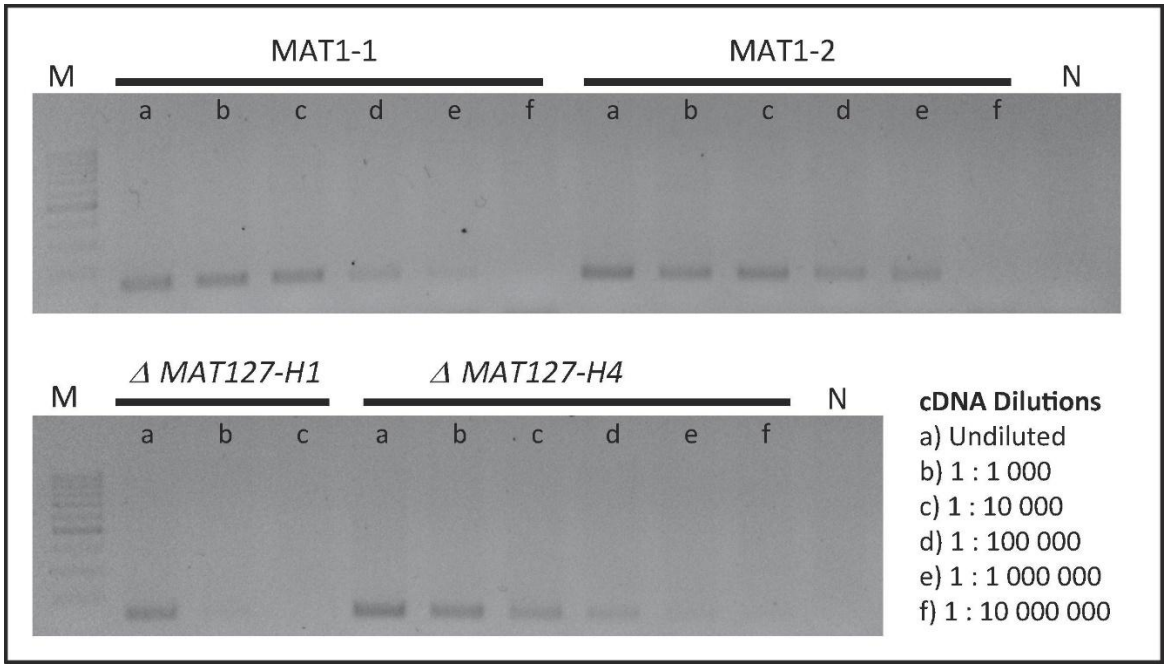

Fig. 6. Expression of the a-pheromone. Transcripts of the a-pheromone receptor were detectable in MAT1-1 and MAT1-2 wild type isolates as well as the two mutant isolates. The semi-quantitative approach used in this study shows that the MAT1-1 isolate expresses the a-pheromone at lower level, with transcripts becoming undetectable at dilutions higher than 1 : 1 000 000, while the pheromone transcript is still detectable at this dilution in the MAT1-2 isolate. Both mutant isolates, *ΔMAT127-H1* and *ΔMAT127-H4*, express the a-pheromone at much lower levels than the wild type isolates, with expression becoming undetectable at dilutions higher than 1 : 10 000 and 1: 1 000 000, respectively. Lanes M and N show the 100 bp molecular marker and negative control, respectively.

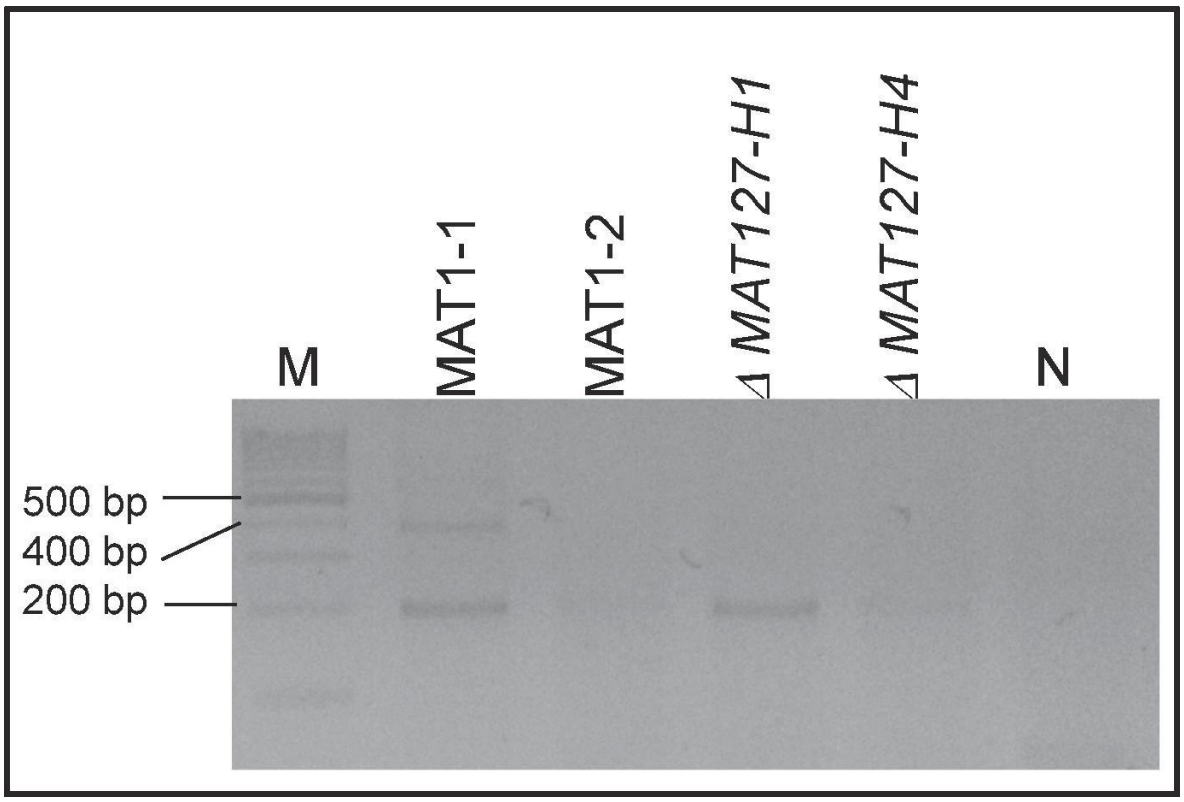

Fig. 7. Expression of the α-pheromone. Transcripts of the **α**-pheromone were detectable in the wild type MAT1-1 isolate but were not detected in the wild type MAT1-2 isolate, as expected. Interestingly, while the *ΔMAT127-H4* mutant showed no evidence of the **α**-pheromone expression, the **α**-pheromone was expressed at detectable levels in the *ΔMAT127-H1* mutant. The larger band in the MAT1-1 lane is the result of non-specific binding due to the repetitive nature of the **α**-pheromone gene sequence. Lanes M and N show the 100 bp molecular marker and negative control, respectively.

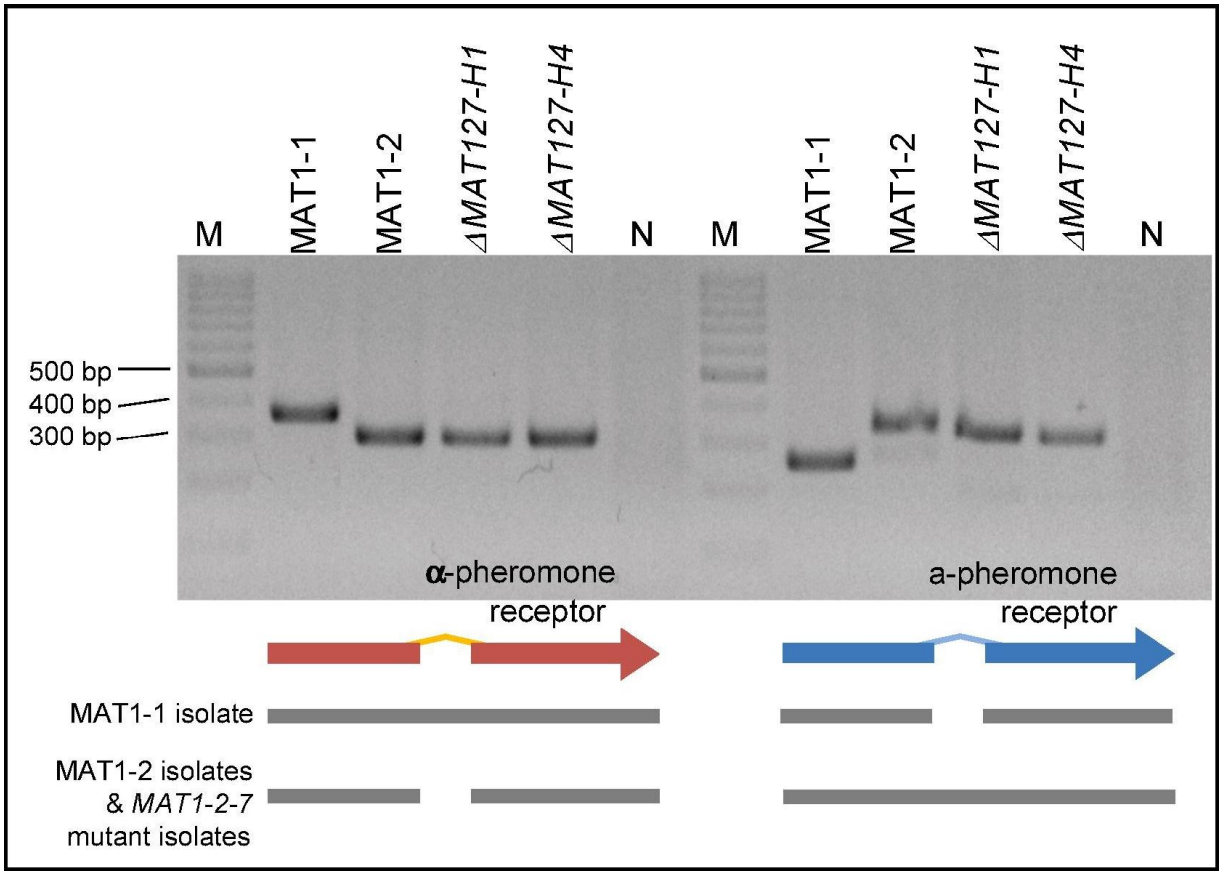

Fig. 8. Mating-type dependant alternative splicing of the pheromone receptors. The two pheromone receptors are spliced differently in the two mating types. In MAT1-1 isolates, the **α**-pheromone receptor mRNA transcript remains unspliced and likely results in a non-functional protein that is incapable of recognizing the **α**-pheromone . In contrast, the MAT1-1 isolates express a splice a-pheromone receptor transcript which, when translated, will produce a functional, seven transmembrane domain protein. The opposite is true for the MAT1-2 isolates, where the **α**-pheromone receptor transcript is correctly spliced, while the a-pheromone receptor remains unspliced, producing a non-functional receptor protein. In both cases, the two mutant isolates produce transcripts identical to that of the wild type MAT1-2 isolates, indicating that the *MAT1-2-7* disruption does not affect the expression or splicing of the pheromone receptor proteins. Lanes M and N show the 100 bp molecular marker and negative control, respectively.

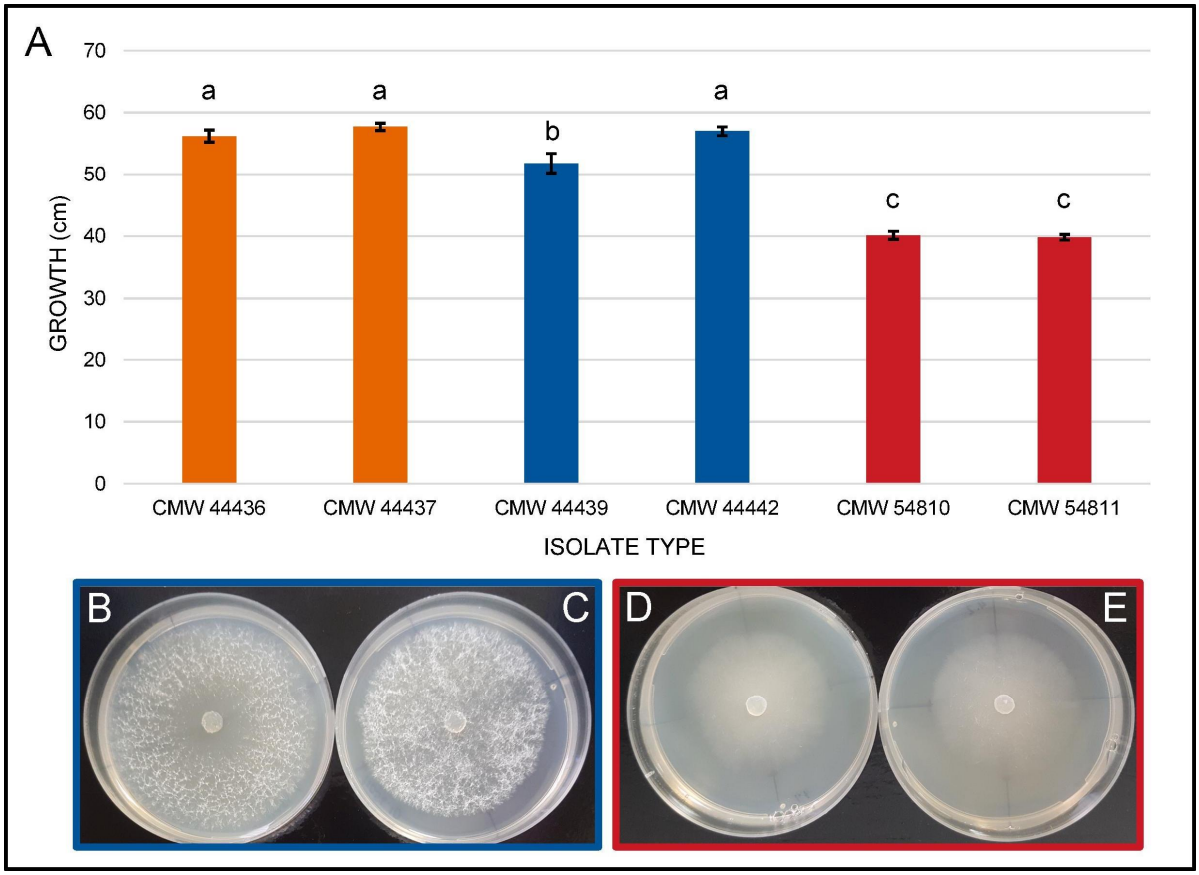

Fig. 9. *MAT1-2-7* truncation leads to a decrease in growth rate and difference in culture morphology. (A) The MAT1-1 isolates (indicated in orange) and the MAT1-2 isolates (indicated in blue) grow significantly faster than the two mutant isolates (indicated in red). (B and C) The two MAT1-2 isolates (CMW 44439 and CMW 44442, respectively) produce aerial mycelia, while (D and E) the mutant isolates (CMW 54810 and CMW 54811, respectively) both produce much smoother, submerged mycelia.